geoconvention
Virtual Event
September 21-23
2020
CSPG • CSEG • CWLS • GAC • MAC • IAH

Offset-to-angle calculations for PS data

Charles Ursenbach and Gary Margrave
TGS Canada

Summary

Comparisons are given for moveout-based offset-to-angle calculation methods for PS data, including an improved method for obtaining the conversion point.

Theory

In the context of AVO analysis, Walden (1991) introduced a quick, approximate method for mapping offsets to angle of incidence for P-wave reflection data of horizontally layered media. It combines the NMO equation, $T_P = (T_{P0}^2 + x^2/v_{P2}^2)^{1/2}$, with the ray-parameter definition, $p = dT_P/dx$, where T_P is PP-reflection traveltime, T_{P0} is zero-offset T_P, x is offset, v_{P2} is the rms P-wave velocity, $p = \sin\theta_P / v_P$ is the ray parameter, θ_P is the P-wave angle at reflection, and v_P is the interval velocity just above the reflector. Together these yield Walden's relation, $\sin\theta_P = xv_P/(T_P v_{P2}^2)$. An identical procedure for SS reflection data yields $\sin\theta_S = xv_S/T_S v_{S2}^2$, where T_S, v_{S2}, v_S, and θ_S are analogues to the P-wave quantities above. This is a significant improvement over the straight ray approximation given by $\sin\theta_P = x/(T_P v_{P2})$.

The same reasoning can be applied to converted-wave reflection data (e.g., Bale et al., 2001). Now the ray parameter is given by dT_C/dx, and we require a PS moveout equation. The simplest such expression, given by Tessmer and Behle (1988), is

$$T_C = \sqrt{T_{C0}^2 + x^2/v_{C2}^2}, \tag{1}$$

where v_{C2}, T_{C0}, are T_C are analogous to v_{P2}, T_{P0} and T_P.

Alternatively, Thomsen (1999) provides a higher order result:

$$T_C = \sqrt{T_{C0}^2 + \frac{x^2}{v_{C2}^2} + \frac{A_4 x^4}{1 + A_5 x^2}}, \quad A_4 = \frac{-(\gamma_2^2 - 1)^2}{4(\gamma_{\text{eff}} + 1)^2(\gamma_0 + 1)v_{C2}^4 t_{C0}^2}, \quad A_5 = \frac{-A_4 v_{C2}^2}{1 - v_{C2}^2/V_{P2}^2} \tag{2}$$

Estimates of the ratios γ_0, γ_2, and γ_{eff} (defined in Thomsen (1999)) can be obtained in the course of converted-wave processing.

A third approach to PS moveout is to note that $T_C = t_P + t_S$ and $x = x_P + x_S$, where t_P and t_S refer to pre- and post-conversion traveltimes, and x_P and x_S refer to portions of the offset before and after the conversion point. Because the pre- and post-conversion legs each possess the same ray-parameter as the full reflected ray, we can in principle define two additional moveout equations, as discussed by Bale et al. (1999):

$$t_P = \sqrt{t_{P0}^2 + x_P^2/v_{P2}^2} \quad \text{and} \quad t_S = \sqrt{t_{S0}^2 + x_S^2/v_{S2}^2}\,. \tag{3), (4)}$$

The new quantities in Eqs 3 and 4 can be obtained from Thomsen (1999), using his Eqs 26-29 for x_P and x_S, Eqs 20 and 22 for t_{P0} and t_{S0}, and Eqs 21 and 23 for v_{P2} and v_{S2}; then t_P and t_S are obtained from Eqs 3 and 4 of this paper. These can be used in dt_P/dx_P and dt_S/dx_S to derive expressions for p.

Eqs 3 and 4 can then be combined to yield a double square root (DSR) moveout expression:

$$T_C = \sqrt{t_{P0}^2 + x_P^2/v_{P2}^2} + \sqrt{t_{S0}^2 + x_S^2/v_{S2}^2} \tag{5}$$

Eqs 1 through 5 yield five possible ray parameter expressions for PS data:

$$p(\text{Tessmer \& Behle}) = \frac{x}{T_C v_{C2}^2} \tag{6}$$

$$p(\text{Thomsen}) = \frac{x}{T_C}\left(\frac{1}{v_{C2}^2} + A_4 x^2 \frac{2 + A_5 x^2}{(1 + A_5 x^2)^2}\right) \tag{7}$$

$$p(\text{P leg}) = \frac{x_P}{t_P v_{P2}^2} \tag{8}$$

$$p(\text{S leg}) = \frac{x_S}{t_S v_{S2}^2} \tag{9}$$

$$p(\text{DSR}) = \frac{x_P}{t_P v_{P2}^2}\frac{dx_P}{dx} + \frac{x_S}{t_S v_{S2}^2}\frac{dx_S}{dx} \tag{10}$$

Any of these can yield $\sin\theta_P$ or $\sin\theta_S$, given an interval velocity estimate at the reflection point, using $\sin\theta_P = pv_P$ or $\sin\theta_S = pv_S$. However, the derivatives in Eq. 10 deserve further comment.

Because $x = x_P + x_S$, the two derivatives must sum to unity. $p(\text{DSR})$ is therefore a weighted average of $p(\text{P leg})$ and $p(\text{S leg})$. If calculated correctly, $p(\text{P leg}) = p(\text{S leg})$, and this provides a key to improved conversion-point calculations. As indicated above, x_P can be estimated from an expression of the form $x_P = xf(x)$, as detailed in Eqs 26-29 of Thomsen (1999). We can then obtain $x_S = x - x_P$. Employed in Eqs 8 and 9, these approximate values, which we will denote $\bar{x}_P$ and $\bar{x}_S$, generally yield slightly different ray parameters. If we define an error δ, where $\bar{x}_P = x_P + \delta$ and $\bar{x}_S = x_S - \delta$, then using Eqs 3-4 and 8-9 we can derive the following first order estimate:

$$\delta = \frac{\bar{p}(\text{P leg}) - \bar{p}(\text{S leg})}{\dfrac{1/\bar{t}_P}{v_{P2}^2 + \bar{x}_P^2/t_{0P}^2} + \dfrac{1/\bar{t}_S}{v_{S2}^2 + \bar{x}_S^2/t_{0S}^2}} \tag{11}$$

A few iterations of using Eq. 11 quickly refines the Thomsen (1999) conversion-point estimate, and the results of Eqs 8-10 converge efficiently to the same value.

Testing

To test the relative merits of Eqs 6, 7, 8 and 10, a simple layered model is described below. In these tests Eq. 10 uses values of x_P and x_S made convergent through use of Eq. 11, and these partial offsets would give identical results in Eqs 8 and 9. For our tests of Eq. 8 however we will use the values of x_P and x_S calculated from Eqs 26-29 of Thomsen (1999), as we observe that they give slightly superior results when used in Eq. 8. Ray-tracing is performed to generate the true incidence (θ_P) and reflection (θ_S) angles for several offsets, then θ_P and θ_S angles are predicted by each of the three methods and compared to exact results. For comparison, straight ray results are also given, which for PS reflections are given by $\sin\theta_P = x_P/(t_P v_{P2})$ and $\sin\theta_S = x_S/(t_S v_{S2})$. Comparable PP reflection results are also shown.

Layer	v_P (m/s)	v_S (m/s)	Thickness (m)
1	1200	320	150
2	1800	880	300
3	2000	1100	200

Table I. Properties of a three-layer model used to test Eqs 6, 7, 8 and 10 and the straight ray approximations.

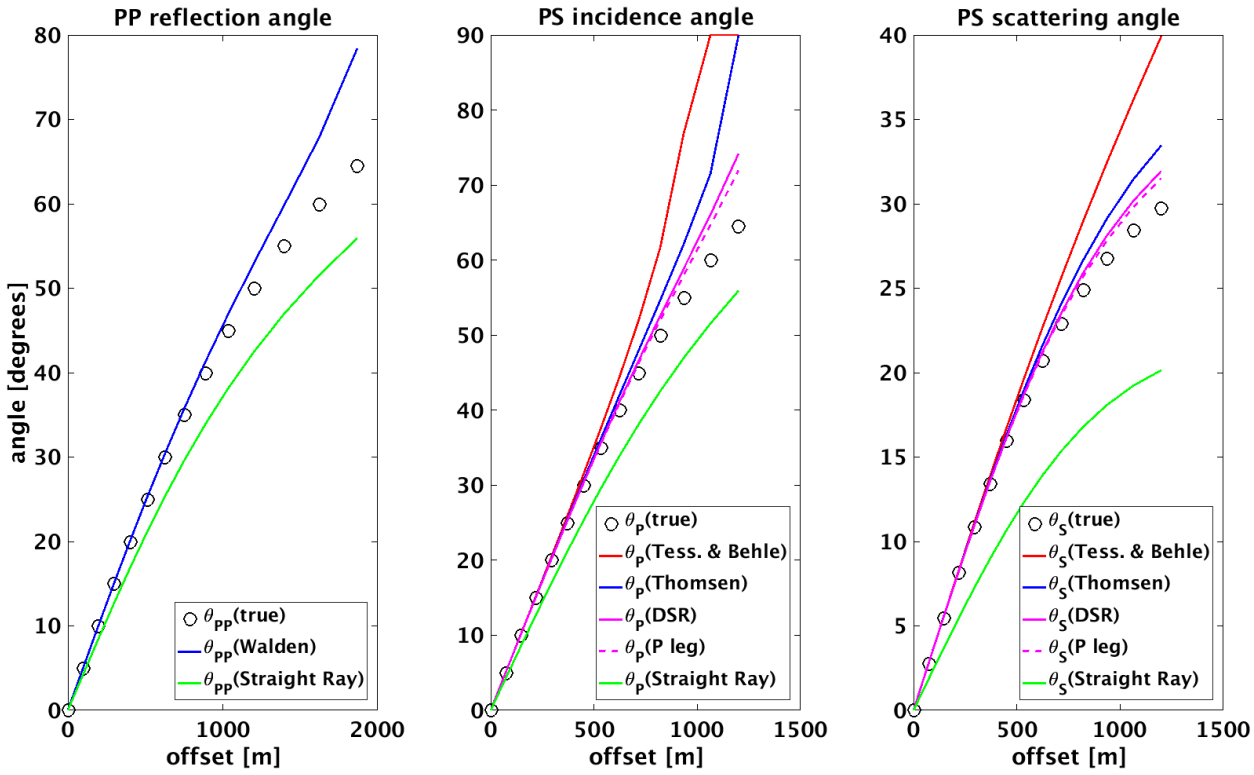

Figure 1. Comparison of results from Eqs 6, 7, 8 and 10 to exact angles obtained from raytracing.

Straight-ray results are poor, as expected, but all bending-ray methods are useful for θ_P < ~30º. At longer offsets, however, Eqs 7, 8 and 10 yield better results than Eq. 6. This is generally true for a wide variety of models, as will be shown in the presentation.

For a more realistic test we apply these methods to PP and PS reflections from a point within a constant thickness blocky model based on well-logs. The model is obtained by 30 m blocking of P and S velocity logs from Hussar, Alberta (Margrave et al., 2011), as shown in Figure 2. Raytracing for reflections at 1500 m depth is illustrated in Figure 3. This gives benchmark traveltimes and angles for a variety of offsets.

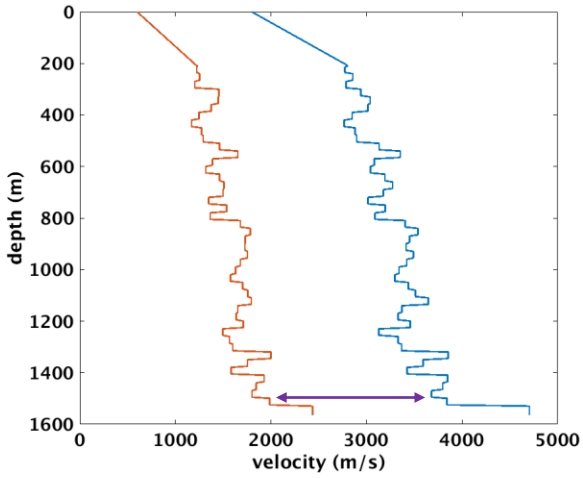

Figure 2. Constant-thickness models obtained by 30 m blocking of P (blue) and S(red) velocity logs from Hussar, Alberta (Margrave et al., 2011). The arrow shows the reflection depth used in raytracing.

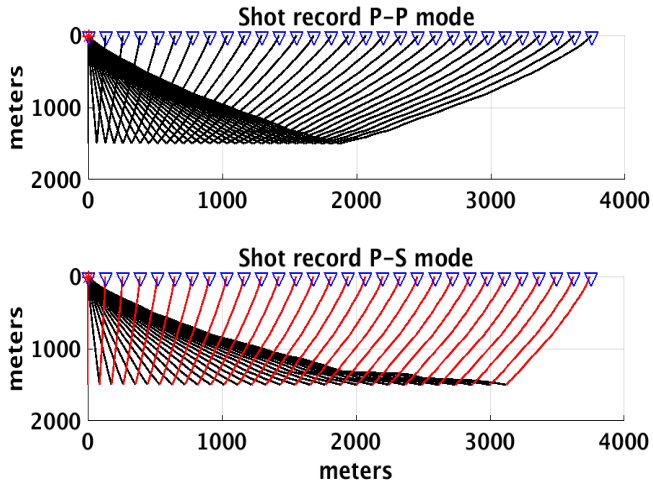

Figure 3. Results of PP and PS raytracing through the model shown in Figure 2. Black lines correspond to P-wave rays and red lines to S-wave rays.

Applying Walden's approximation and Eqs 6, 7, 8 and 10 yields the results in Figure 4 below.

Discussion

It is clear from results that we can improve upon the Tessmer and Behle expression when it comes to converting offsets to angle. Eq. 7, based on the Thomsen (1999) moveout gives accuracy for PS data comparable to the Walden expression for PP data. (Other PS moveout expressions of a form similar to Eq. 2 have also been suggested (e.g., Cheret et al., 2000; Li, 2003).) Eqs 8-10 provide greater accuracy than Eq. 7 when supplied with consistent x_P and x_S values. Eq. 8 performs even better with more approximate x_P and x_S values. We assume that it partially corrects for a bias inherent in underlying theory, a bias which is opposite to that in the straight ray method. While none of these expressions is adequate at the highest angles, the more accurate expressions enable use of higher incidence angles than can be accessed using the Tessmer and Behle expression alone.

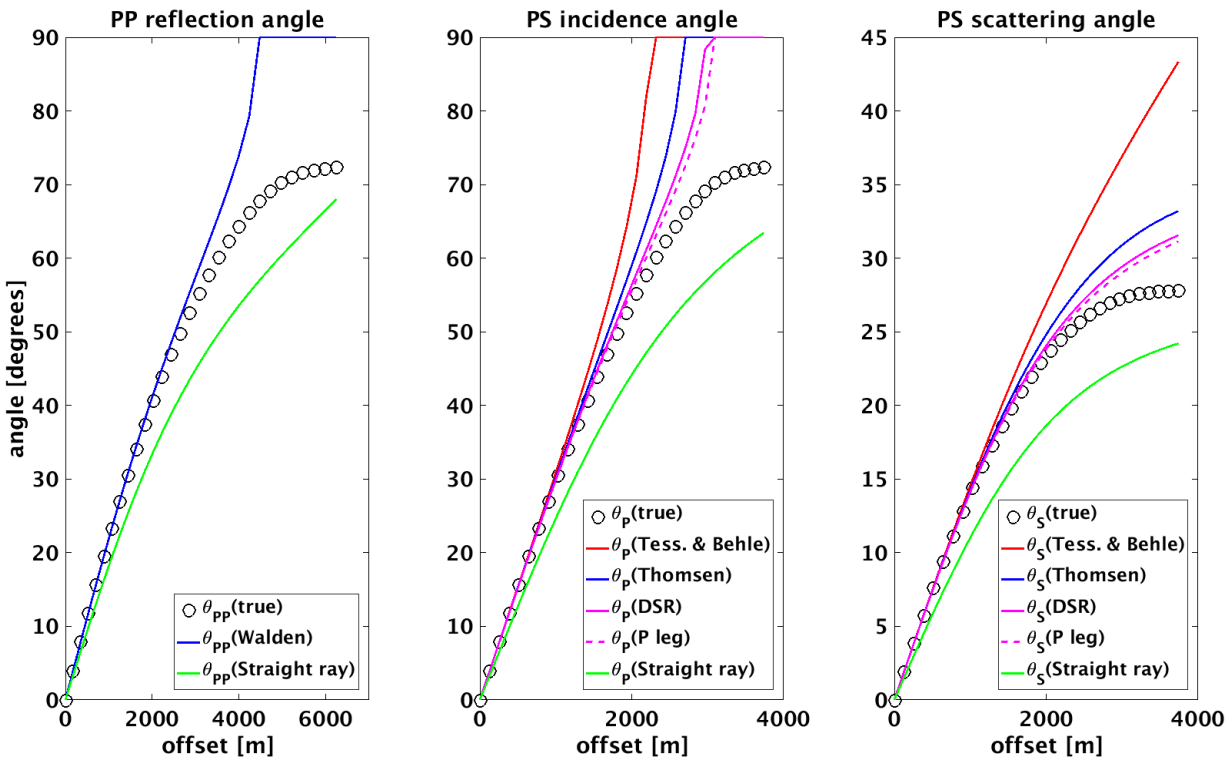

Figure 4. Comparison of "true" incidence and reflection angles obtained from raytracing with estimates obtained from approximate ray expressions described in this work.

Novel Contribution

Possible methods for converted-wave offset-to-angle calculations have been tested and compared. A method is given for refining the conversion point used in some of these. One advantage of PS surveys is their ability to generate large incidence angles with moderate offsets. Methods such as those studied here will help us to capitalize on larger angles in multicomponent AVO and inversion.

References

Bale, R., S. Leaney and G. Dumitru, 2001, SEG Technical Program Expanded Abstracts: 235-238.
Cheret, T., R. Bale and S. Leaney, 2000, SEG Technical Program Expanded Abstracts: 1181-1184.
Li, X.-Y., 2003, SEG Technical Program Expanded Abstracts: 805-808.
Margrave, G. F., L. Mewhort, T. Phillips, M. Hall, M. B. Bertram, D. C. Lawton, K. Innanen, K. W. Hall and K. Bertram, 2011, The Hussar low-frequency experiment: CREWES Research Report Vol. 23.
Tessmer, G. and A. Behle, 1988, Geophysical Prospecting, **36**, 671-688
Thomsen, L., 1999, Geophysics, **64**, 678-690.
Walden, A. T., 1991, Geophysical Prospecting, **39**, 915-942.